

# Low thermal conductivity in amorphous rare-earth-silicon alloy thin films

B. L. ZINK<sup>1,2</sup>, B. REVAZ<sup>1</sup> and F. HELLMAN<sup>1</sup>

<sup>1</sup> *Department of Physics, University of California, San Diego  
La Jolla, California 92093*

<sup>2</sup> *Current Address: National Institute of Standards and Technology, 325 Broadway MS  
814.03, Boulder, CO 80305*

PACS. 65.60.+a – Thermal properties of amorphous solids and glasses: heat capacity, thermal expansion, etc..

PACS. 66.70.+f – Nonelectronic thermal conduction and heat-pulse propagation in solids; thermal waves.

**Abstract.** – We report thermal conductivity and specific heat measurements of amorphous gadolinium-silicon and yttrium-silicon alloy thin films from 4–100 K. The thermal conductivity is an order of magnitude smaller than other disordered solids at low temperatures and does not show the usual plateau near 10–50 K, though the specific heat does show the clear peak in the vibrational spectrum which in amorphous materials is usually linked to the plateau. We attribute the extremely low thermal conductivity and suppression of the expected plateau to heavy rare-earth ions rattling in Si cages which increase phonon scattering and decrease thermal conductivity, similar to effects seen in filled skutterudites but found here in an amorphous structure.

*Introduction.* – Despite a long history of study, the thermal properties of amorphous solids remains an active field with a number of unresolved issues [1, 2, 3, 4]. A very broad range of amorphous solids have similar thermal conductivity,  $k$ , suggesting that some rather universal phenomenon is at work. The best current description is that below 1 K,  $k \propto T^{1.8}$  as a result of scattering off two-level tunneling states (TLS) of uncertain physical origin [5]. These tunneling systems also contribute a linear term to the specific heat,  $C$ , at these temperatures. Above 2 K,  $k$  crosses over from the  $T^{1.8}$  dependence to a plateau, followed by a gradual continuing rise. This plateau is typically seen between 10 and 50 K, where a nearly ubiquitous peak in  $C/T^3$ , also occurs. These phenomena have been shown to be related to scattering of phonons from a high density of local vibrational modes.

There has been some success explaining both the  $C/T^3$  peak and the  $k$  plateau within the general concept of a soft potential model and/or interacting defects, which attempts to fit these phenomena in a single model together with the tunneling states which dominate at  $T < 2$  K. These modeling efforts are still controversial and the details of the models and the underlying microscopic mechanisms are not yet universally accepted. Above 30 K, Slack's model of a minimum thermal conductivity,  $k_{min}$ , somewhat successfully predicts  $k$  for several

amorphous solids [6]. This parameter-free model is based on a random walk between Einstein oscillators of various sizes and significantly underestimates  $k$  at low temperatures where the mean free path exceeds the dominant phonon wavelength [2].

Vapor deposition techniques such as sputtering and e-beam evaporation allow a wide range of amorphous materials to be made, though measurement of the thermal properties of the resulting thin films is difficult. For example in specific heat or thermal conductivity measurements, the contribution of the sample is normally small compared to that of the solid substrate on which the film is condensed. Measurements of  $C$  and  $k$  from 2 – 300 K of thin films are possible with a Si-N membrane microcalorimeter [7, 8], where a 2000 Å thick membrane is used to reduce the contribution from the elements used to support and measure the thin film.

Silicon and germanium are two materials that can only be made in amorphous form by vapor deposition. These tetrahedrally-bonded elemental amorphous solids have been studied in detail, partly because some theories predict an absence of tunneling states in this overconstrained network [9]. This prediction has been difficult to prove in studies of thermal properties below 1 K because of the difficulty of measurement techniques and an apparent strong dependence on the growth method and quality of the sample (for a recent review see [10]). The current view, clarified by measurements of the internal friction of a range of  $a$ -Si films, is that the perfection of the tetrahedrally bonded network determines the concentration of tunneling systems, which can be varied with the concentration of hydrogen in the material [10]. Note that no direct measurement of  $k$  for  $a$ -Si has been reported for  $T < 1$  K. Measurements of thermal properties of  $a$ -Si in the temperature range where the  $k$  plateau and  $C/T^3$  peak are expected have been limited to two studies of sputtered  $a$ -Si [11, 12], which show the plateau and peak occurring at similar temperatures, as expected for amorphous materials. The only departure from typical amorphous behavior noted by these authors is that the  $C/T^3$  peak in  $a$ -Si occurs at a temperature ( $T_{max} = 30$  K) closer to that seen in crystalline Si ( $T_{max} = 39$  K) than seen in other amorphous systems.

Amorphous gadolinium-silicon ( $a$ -Gd $_x$ Si $_{1-x}$ ), where e-beam co-deposition is used to form a film consisting of an  $a$ -Si network with heavy rare-earth ion dopants, has shown many phenomena related to the interaction between local Gd magnetic moments and conduction electrons including a very large negative magnetoresistance at low temperatures [13, 14]. Recent computational and experimental results begin to shed some light on the structure of  $a$ -Gd $_x$ Si $_{1-x}$  and its non-magnetic analog, yttrium-silicon. Local density functional theory simulations of  $a$ -Y $_x$ Si $_{1-x}$  suggest that Y $^{3+}$  ions are surrounded by low-coordinated Si, leaving them in a “cage” of dangling bonds [15]. X-ray absorption fine structure (XAFS) experiments on  $a$ -Gd $_x$ Si $_{1-x}$  using both the Si and Gd absorption edges give a similar picture, with Si atoms as nearest-neighbors to the Gd ions and no clustering [16]. The XAFS studies also indicate that neither the Si coordination number nor the Gd-Si distance changes with Gd composition, suggesting a Si cage but no dangling bonds. Structural measurements including XAFS (on  $a$ -Y-Si) and electron spin resonance are continuing in order to resolve this discrepancy. Cages in  $a$ -Gd $_x$ Si $_{1-x}$  are further supported by calculations using the full potential linearized augmented plane wave (FLAPW) method [17]. Both XAFS and RBS measurements indicate atomic densities consistent with pore-free films. The thermal conductivity of amorphous materials with heavy ion impurities has yet to be studied in the 2 – 300 K temperature range to the best of our knowledge.

In this letter we present thermal conductivity and specific heat measurements of  $a$ -RE-Si films from 3.5 – 100 K. We demonstrate that  $k$  is dominated by phonons by comparison with  $k_{el}$  calculated from the electrical conductivity. We then compare  $k$  to published results for several other amorphous solids and the calculated  $k_{min}$ , which shows  $a$ -RE-Si to have a very low thermal conductivity and no visible plateau above 3 K. Finally we present the specific

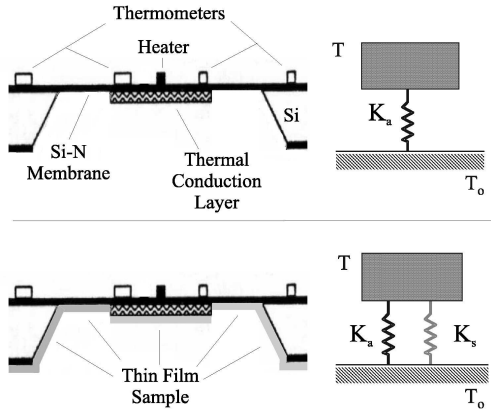


Fig. 1

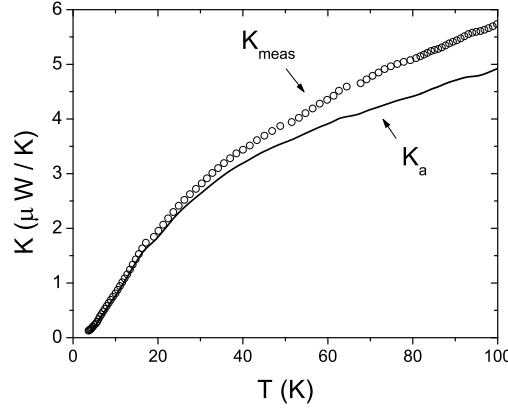


Fig. 2

Fig. 1 – A side-view schematic of the calorimeter with a 2d thermal model of the system. Before deposition of the sample the conductance  $K_a$  links the heated central  $0.25 \text{ cm} \times 0.25 \text{ cm}$  area at  $T_o + \Delta T$  to the Si frame at  $T_o$ . After a thin film sample is deposited on the entire bottom surface of the membrane, the link becomes  $K_{meas} = K_a + K_s$ .  $K_s$  is then determined by subtracting  $K_a$ .

Fig. 2 –  $K$  vs.  $T$ .  $K_a$  is the background thermal link,  $K_{meas}$  includes the  $1200 \text{ \AA}$  *a*-Gd-Si film with 14% Gd.

heat,  $C$ , of *a*-Y-Si and compare the peak in the vibrational spectrum to that seen in vitreous silica and *a*-Si.

*Experiment.* – We have recently extended our technique for measuring specific heat using Si-N membrane-based microcalorimeters [7] to measuring the thermal conductivity of thin films [18]. The microcalorimeter’s thermal link,  $K_a$ , consists of contributions from the  $2000 \text{ \AA}$  thick Si-N membrane and the  $500 \text{ \AA}$  thick Pt heater and thermometer leads. When a thin film sample is deposited on the membrane as shown in Fig. 1, heat is also conducted through this film. For a broad range of temperatures, we determine the contribution of the sample film,  $K_s$ , by subtracting  $K_a$  from the values measured after sample deposition,  $K_{meas}$ . The thermal conductivity of the film is determined using the thickness measured with a Dektak IIA profilometer and a 2d geometry factor resulting from numerical simulations of the heat flow in the calorimeter [19].

Using this technique we previously measured a  $200 \text{ \AA}$  Au film and a  $2000 \text{ \AA}$  Pb film in its superconducting and magnetic field induced normal states [8, 18]. We also determined  $k$  for the Si-N membrane itself which agrees well with existing data on these type of membranes [20]. Further details of the technique [18, 8] and the e-beam deposition of the *a*-RE-Si samples [13, 21] appear elsewhere.

*Results.* – Figure 2 shows the measured thermal link of the “empty” calorimeter,  $K_a$ , and the calorimeter with  $1200 \text{ \AA}$  *a*-Gd-Si (14 at. % Gd),  $K_{meas}$ . The thermal conductance of the calorimeter is increased only slightly by the addition of the sample despite the fact that its thickness is half that of the *a*-Si-N membrane. Fig. 3 shows  $k$  vs.  $T$  for 10 at. % Gd, 14 at. % Gd and 12 at. % Y films. The error bars shown at 90 K and 20 K were determined assuming 2% error on both  $K_a$  and  $K_{meas}$  and a  $\pm 50 \text{ \AA}$  error on the thickness. The three samples have the same thermal conductivity within error bars at all  $T$ .

The inset in Fig. 3 is a log-log plot which compares the measured values of  $k$  in  $\text{mW/cmK}$

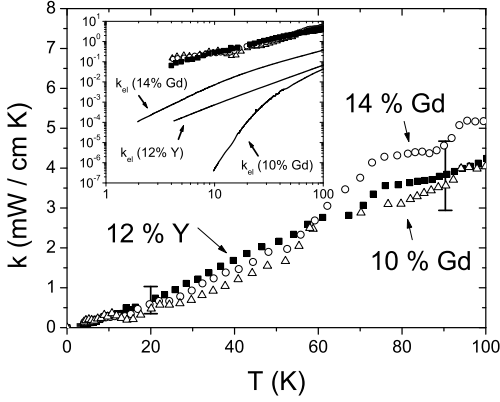


Fig. 3

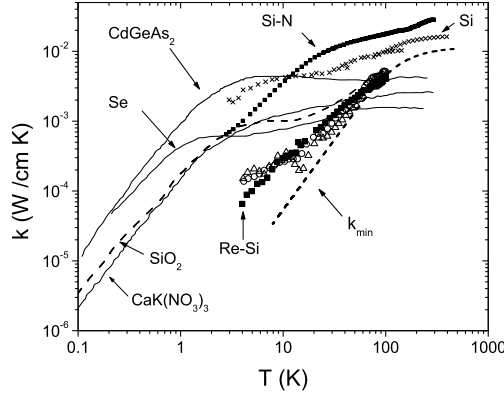


Fig. 4

Fig. 3 –  $k$  (mW/cmK) vs.  $T$  for three  $a$ -RE-Si samples. INSET:  $\log k$  vs.  $\log T$  showing measured  $k$  and the estimated electronic contribution,  $k_{el} = \sigma L_0 T$ .

Fig. 4 –  $\log k$  vs.  $\log T$  plot comparing results for several amorphous solids.  $a$ -RE-Si has much lower  $k$  at low  $T$ , and is reduced by at least a factor of 2 below  $a$ -Si at high  $T$ , where it agrees well with  $k_{min}$ .

to the contribution of electrons,  $k_{el}$ , calculated from electrical conductivity,  $\sigma$  [13], via the Wiedemann-Franz law,  $k_{el}/\sigma = L_0 T$ , with  $L_0 = 2.44 \times 10^{-8} \text{ W} \cdot \Omega/\text{K}^2$ . For  $a$ -RE-Si the measured values of  $k$  are at least an order of magnitude larger than the  $k_{el}$  values, with no strong suppression in the  $k$  of the Gd-Si films. This indicates that the thermal conductivity is totally dominated by phonons at even our lowest measured temperatures. We also measured the Gd samples in magnetic fields up to 8 T and found less than 1% difference in  $k$  below 20 K, where the electrical conductivity of a similar sample changes by orders of magnitude. We observed similar insensitivity to magnetic field at all measured  $T$ , which precludes the existence of enhanced electron-phonon or magnon-phonon coupling in this material.

Figure 4 compares our measured  $a$ -RE-Si  $k$  values to several other amorphous solids on a log-log plot. The solid squares are the values for the  $a$ -Si-N which forms the membrane [20]. The dashed line is the result for vitreous silica [1], the three smooth solid lines are representative amorphous solids which span the range of  $k$  (vitreous selenium, CdGeAs<sub>2</sub> and CaK(NO<sub>3</sub>)<sub>3</sub> [2]), and the  $\times$ 's show  $a$ -Si [22, 11, 23]. The thermal conductivity of  $a$ -RE-Si is an order of magnitude smaller than  $a$ -Si below 30 K and is at least a factor of 5 lower than even  $a$ -Se at 4 K. From 50 – 100 K,  $k$  approaches the values for vitreous silica but remains much smaller than  $a$ -Si and  $a$ -Si-N.

Turning now to measurements of the specific heat, Fig. 5 shows  $C/T^3$  vs.  $T$  (in J/gK<sup>4</sup>) on a log-log plot for  $a$ -Y-Si (13% Y) (solid squares) [24],  $a$ -Si (dotted line) [12] and vitreous silica (dashed line) [1].  $a$ -Y<sub>x</sub>Si<sub>1-x</sub> for a broad range of  $x$  have very similar specific heat above 60 K, and all show the maxima in  $C/T^3$  shown here. Samples with larger  $x$  have electronic terms,  $\gamma T$  (which appear as  $1/T^2$  on this plot), and an additional contribution to  $C$  occurs in samples near the M-I transition [24, 8]. We have previously reported the specific heat of  $a$ -Gd<sub>x</sub>Si<sub>1-x</sub>, which is similar to values for  $a$ -Y<sub>x</sub>Si<sub>1-x</sub> above 60 K, but is dominated at lower temperatures by a large peak associated with magnetic degrees of freedom [25, 21, 8]. The short dotted line near the  $C/T^3$  axis indicates the low temperature value of a Debye specific heat calculated from the sound velocity in vitreous silica [1]. The short solid line is a similar Debye specific

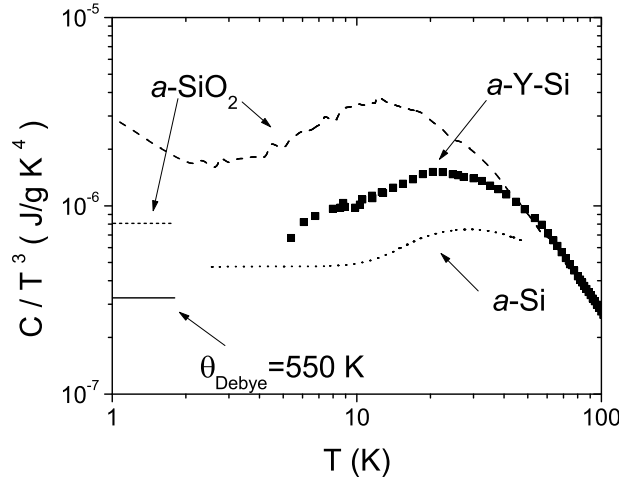


Fig. 5 –  $C/T^3$  vs.  $T$  for *a*-Y-Si (12 at. % Y), *a*-Si [12] and *a*-SiO<sub>2</sub> [1]. All show the peak characteristic of amorphous solids which scales as expected. *a*-Y<sub>x</sub>Si<sub>1-x</sub> with other values of  $x$  all show similar maxima. *a*-Gd<sub>x</sub>Si<sub>1-x</sub> (not shown) has very large contributions from magnetic degrees of freedom which mask the peak in  $C/T^3$  [25, 8]. The reported Debye temperature of *a*-Si is  $528 \pm 20$  K [12].

heat function calculated for *a*-Y-Si using the atomic density,  $n = 5 \times 10^{22} \text{ cm}^{-3}$ , determined from RBS measurements and assuming a typical sound velocity,  $v = 5 \times 10^5 \text{ cm/s}$ , giving  $\Theta_D = 550$  K. These values calculated from sound velocities estimate the contribution from phonons which carry heat. The measured  $C$  for both materials exceeds this propagating-mode estimation, indicating large contributions from localized, non-propagating vibrational modes.

The broad peak in  $C/T^3$  is a ubiquitous feature in amorphous solids (which is also seen in crystalline materials that have a flat branches in the vibrational dispersion relation) and is related to the “boson peak” seen in neutron scattering [26, 4]. For a broad range of materials, including the vitreous silica, *a*-Si and *a*-Y-Si shown in Fig. 5, the height of the peak,  $P_c$ , increases as its temperature,  $T_{max}$ , decreases, so that  $P_c \propto T_{max}^{-1.6}$  [26]. The upturn below 2 K in  $C/T^3$  for the vitreous silica is the large linear term in  $C$  due to two-level tunneling systems [5]. As expected, there is little sign of either an electronic or a TLS linear term in *a*-Y-Si in the temperature range we studied; it would likely be found at lower temperatures.

*Discussion.* – The most important result of these experiments is that the thermal conductivity of *a*-RE-Si is dramatically smaller than other dense amorphous solids at low  $T$ , and is well below *a*-Si at all  $T$ . This result is evident even in Fig. 2 where the addition of  $\approx 1200$  Å of material, (more than half of the thickness of the Si-N membrane) increases the thermal link,  $K_{meas}$  by only 15% at 4 K, (and only 25% at 100 K).

One tool commonly used to help understand thermal conductivity of amorphous solids is Slack’s model for the minimum conductivity [6, 2]. In this model heat is transported through a material by a random walk between strongly damped Einstein oscillators of various sizes. The dotted line shown in Fig. 4 is the result for  $k_{min}$  again using  $n = 5 \times 10^{22} \text{ cm}^{-3}$  and  $v = 5 \times 10^5 \text{ cm/s}$ .  $k_{min}$  agrees well with the measured  $k$  at high temperatures and, as expected, underestimates  $k$  at low temperatures. This high  $T$  agreement with  $k_{min}$  actually indicates a comparatively low  $k$ , as the measured values for most amorphous solids are larger than  $k_{min}$  at all  $T$ . To make a quantitative comparison with either a tunneling model or the

soft potential model would require more data below 2 K, in order to establish the crossover temperature from tunneling to vibrational modes. It is clear however from the data in Fig. 4 that the usual plateau in  $k$  (expected near the peak in  $C/T^3$  at  $\sim 25$  K) is not present. We suggest therefore that  $k$  is suppressed in this material below the normal amorphous material temperature dependence for  $T < 30$  K by an additional strong scattering mechanism.

Filled skutterudites are materials which have low thermal conductivity while maintaining a large electrical conductivity, making them good thermoelectric materials [27]. Here heavy (often rare-earth) ions are substituted into large sites or "cages" in the skutterudite crystal structure. The heavy ions exhibit strongly anharmonic rattling motion, dramatically increasing phonon scattering and reducing the thermal conductivity. Filled skutterudites can have an order of magnitude smaller  $k$  than the unfilled structures at room temperature, with even larger differences at low  $T$  [27]. We propose that a similar mechanism occurs in  $a\text{-RE}_x\text{-Si}_{1-x}$ : rare-earth ions in Si "cages" rattle anharmonically and reduce the phonon mean free path and thermal conductivity.

The rattling modes in filled skutterudites typically also cause an additional low energy Einstein contribution to the specific heat [28] and can cause softening of the entire lattice [29] when compared to the unfilled structures. Below 60 K the specific heat of  $a\text{-Y-Si}$  over a broad range of composition is larger than reported values for  $a\text{-Si}$  [12] (as shown for one composition in Fig. 5). Because the electronic contribution to the specific heat is small in  $a\text{-Y-Si}$  [8,24], this additional specific heat is likely due to vibrational states and could include the contributions of the rattling modes.

Below 10 K surface scattering of phonons can substantially alter thermal transport in these Si-N membranes [20] and introduce errors in determining the contribution of the sample at low  $T$  [8]. However, the membranes used for this study are in a diffuse surface scattering limit, where the effect of surface scattering should be small, and if present would cause an underestimation of the contribution of the membrane to  $K_a$  and therefore cause an *overestimation* of the already very low thermal conductivity of the sample film. In addition, estimation of the phonon mean free path in the  $a\text{-Re-Si}$  films using the Debye specific heat of propagating modes indicates that at all temperatures the mean free path is less than the thickness of the films. This suggests that surface scattering is not a limiting factor.

*Conclusion.* – In summary, we have measured the thermal conductivity of three  $a\text{-RE-Si}$  samples, which show remarkably low values compared to typical amorphous solids at low  $T$ . Though very low thermal conductivities are seen in porous solids, such low values have not previously been observed in a fully dense amorphous material [16]. Experimental and theoretical evidence suggests that in  $a\text{-RE-Si}$  the heavy rare earth ions are contained in Si cages. We suggest that localized vibrations of these heavy rare earth ions strongly scatter phonons, reducing the thermal conductivity, similar to the "rattling" seen in filled skutterudites. This scattering suppresses the usual plateau in  $k$  which would be expected near 10–25 K, based on the  $C/T^3$  peak, suggesting that the phonon mean free path is limited by the rattling cage modes rather than the usual vibrational modes associated with the  $C/T^3$  peak. Future work will investigate the tunneling regime in heavy-ion doped amorphous systems by measuring  $k$  and  $C$  below 1 K as well as the internal friction.

*Acknowledgments.* – We would like to thank B. B. Maranville, M. Liu and M. Wong for the RBS measurements, D. Cahill, B. Pohl, A. Migliori and R. Dynes for fruitful discussions, J. J. Cherry for the profilometry, and the NSF and LANL for support.

## REFERENCES

- [1] R. C. Zeller and R. O. Pohl, Phys. Rev. B **4**, 2029 (1971).
- [2] D. G. Cahill and R. O. Pohl, Ann. Rev. Phys. Chem. **39**, 93 (1988).
- [3] R. O. Pohl, X. Liu, and E. Thompson, Reviews of Modern Physics **74**, 991 (2002).
- [4] M. A. Ramos and U. Buchenau, in *Tunneling systems in amorphous and crystalline solids*, edited by P. Esquinazi (Springer-Verlag, Berlin, 1998).
- [5] P. W. Anderson, B. I. Halperin, and C. M. Varma, Philos. Mag. **25**, 1 (1972).
- [6] G. A. Slack, Solid State Physics **34**, 1 (1979).
- [7] D. W. Denlinger, E. N. Abarra, K. Allen, P. W. Rooney, M. T. Messer, S. K. Watson, and F. Hellman, Rev. Sci. Instrum. **65**, 946 (1994).
- [8] B. L. Zink, Ph.D. thesis, University of California, San Diego, 2002.
- [9] W. A. Phillips, Journal of Low Temperature Physics **7**, 351 (1972).
- [10] X. Liu and R. O. Pohl, Physical Review B **58**, 9067 (1998).
- [11] G. Pompe and E. Hegenbarth, Phys. Status Solidi B **147**, 103 (1988).
- [12] M. Mertig, G. Pompe, and E. Hegenbarth, Solid State Communications **49**, 369 (1984).
- [13] F. Hellman, M. Q. Tran, A. E. Gebala, E. M. Wilcox, and R. C. Dynes, Phys. Rev. Lett. **77**, 4652 (1996).
- [14] P. Xiong, B. L. Zink, S. I. Applebaum, F. Hellman, and R. C. Dynes, Phys. Rev. B **59**, R3929 (1999).
- [15] V. Meregalli and M. Parrinello, Solid State Communications **117**, 441 (2001).
- [16] D. Haskel, J. W. Freeland, J. Cross, R. Winarski, M. Newville, and F. Hellman, Physical Review B **67**, 115207 (2003).
- [17] R. Wu (unpublished).
- [18] B. L. Zink, B. Revaz, J. J. Cherry, and F. Hellman, submitted to RSI (unpublished).
- [19] B. Revaz, D. O'Neil, L. Hull, and F. Hellman, Review of Scientific Instruments **74**, 4389 (2003).
- [20] B. L. Zink and F. Hellman, *SSC* (in press) (unpublished).
- [21] B. L. Zink, V. Preisler, D. R. Queen, and F. Hellman, Physical Review B **66**, 195208 (2002).
- [22] D. G. Cahill, M. Katiyar, and J. R. Abelson, Phys. Rev. B **50**, 6077 (1994).
- [23] D. G. Cahill, H. E. Fischer, T. Klitsner, E. T. Swartz, and R. O. Pohl, J. Vac. Sci. Technol. A **7**, 1259 (1989).
- [24] B. L. Zink and F. Hellman, in final preparation (unpublished).
- [25] B. L. Zink, E. Janod, K. Allen, and F. Hellman, Phys. Rev. Lett. **83**, 2266 (1999).
- [26] X. Liu and H. v. Lohneysen, Europhysics Letters **33**, 617 (1996).
- [27] G. S. Nolas, D. T. Morelli, and T. M. Tritt, Annu. Rev. Mater. Sci. **29**, 89 (1999).
- [28] A. Grytsiv, P. Rogl, S. Berger, C. Paul, H. Michor, E. Bauer, G. Hilscher, C. Godart, P. Knoll, M. Musso, W. Lottermoser, A. Saccone, R. Ferro, T. Roisnel, and H. Noel, Journal of Physics Condensed Matter **14**, 7071 (2002).
- [29] E. Bauer, A. Galatanu, H. Michor, G. Hilscher, P. Rogl, P. Boulet, and H. Noel, European Physical Journal B **14**, 483 (2000).